신경망기법을 이용한 구조물 접합부의 손상평가
Structural Joint Damage Estimation by Neural Networks Incorporating Advanced Techniques

이진학* 윤정방** 방은영***
Yi, Jinhak* Chung-Bang Yun** Eun-Young Bahng***

국문요약

신경망기법을 이용한 구조물접합부의 손상평가기법을 제안하였다. 신경망기법의 성능을 개선하기 위하여 노이즈첨가학습을 수행하였으며, 효과적인 손상평가를 위하여 부분구조추정법 및 data perturbation scheme을 도입하였다. 10층 프레임구조물에 대한 수치해석과 2층 프레임구조물에 대한 실험연구를 통하여 제안기법을 검증하였다. 계측지점이 부분구조로 제한되고, 계측자료가 노이즈를 포함하는 경우에도 제안기법이 효과적으로 적용될 수 있음을 알 수 있었으며, 실험을 통하여 실제 구조물에 대한 제안기법의 적용성을 평가할 수 있었다.

1. Introduction

Most of the damage assessment methods for large-scale frame structures consider the element-level damages, however, the beam-to-column connections in a steel structure are more susceptible to damages than the other parts of the structure. However, only a few studies have been reported on the estimation of the joint damages of large-scale steel structures. This research deals with the modeling of damages for the beam-to-column connections of a steel frame structure and the identification of the joint damages based on the modal data using neural networks technique. The rotational stiffness of a beam-to-column connection of a frame structure is represented by a zero-length rotational spring at the end of the beam element. The severity of the joint damage is defined as the reduction ratio of the connection fixity factor. In this study, three advanced techniques are incorporated to overcome the difficulties in the damage detection processes. The noise-injection learning algorithm is used to reduce the effects of the noise in modal data. The data perturbation scheme is employed to reduce the uncertainty and to assess the confidence level of the estimated damage. The concept of the substructural identification is used for the localized damage assessments in a large structure.

2. Modeling of Semi-Rigid Connections and Joint Damages

The semi-rigid connections can be modeled by zero-length rotational springs at the ends of a beam as Figure 1. The stiffness matrix of a beam element with semi-rigid connections at the ends can be obtained for the degrees of freedom at the external nodes, $\{u\} = < v_1, \theta_1, v_2, \theta_2 >^T$, as

* 한국과학기술원 박사과정
** 한국과학기술원 교수, 정회원
*** 동양대학교 전임강사

$$[k]=\begin{bmatrix} \frac{12EI}{L^3}\left(\frac{f_1}{f_7}\right) & & \textit{symmetric} & \\ \frac{6EI}{L^2}\left(\frac{f_2}{f_7}\right) & \frac{4EI}{L}\left(\frac{f_3}{f_7}\right) & & \\ -\frac{12EI}{L^3}\left(\frac{f_1}{f_7}\right) & -\frac{6EI}{L^2}\left(\frac{f_2}{f_7}\right) & \frac{12EI}{L^3}\left(\frac{f_1}{f_7}\right) & \\ \frac{6EI}{L^2}\left(\frac{f_6}{f_7}\right) & \frac{2EI}{L}\left(\frac{f_5}{f_7}\right) & -\frac{6EI}{L^2}\left(\frac{f_6}{f_7}\right) & \frac{4EI}{L}\left(\frac{f_4}{f_7}\right) \end{bmatrix} \tag{1}$$

where the parameters f_i's are defined using the joint fixity factors (γ_1 and γ_2) as: $f_1=\gamma_1+\gamma_2+\gamma_1\gamma_2$, $f_2=\gamma_1(2+\gamma_2)$, $f_3=3\gamma_1$, $f_4=3\gamma_2$, $f_5=3\gamma_1\gamma_2$, $f_6=\gamma_2(2+\gamma_1)$, and $f_7=4-\gamma_1\gamma_2$, in which the joint fixity factors are defined using the rotational stiffnesses of the end springs and the beam (k_{r_1}, k_{r_2} and $3EI/L$) as

$$\gamma_1=1/\left(1+\frac{3EI}{Lk_{r_1}}\right) \quad , \quad \gamma_2=1/\left(1+\frac{3EI}{Lk_{r_2}}\right) \quad , \qquad 0\le\gamma_1 \textit{ and } \gamma_2\le 1.0 \tag{2}$$

In this study, the joint damage severity at node i (α_i) is defined by the reduction ratio of the fixity factor of the damaged joint(γ_i) to the fixity of the intact joint($\gamma_{0,i}$) as

$$\alpha_i=1-\gamma_i/\gamma_{0,i} \quad , \quad 0\le\alpha_i\le 1.0 \tag{3}$$

where the fixity factor of the intact joint ($\gamma_{0,i}$) can be estimated using the intact joint rotational stiffness ($k_{r0,i}$) which may be obtained on the basis of available database or experimental results.

3. Neural Networks for Joint Damage Estimation

In this study, a popular neural networks model called a multi-layer perceptron (MLP) or a back-propagation neural networks (BPNN) is used for the identification of the damage parameters(see Figure 2). The concept of the substructural identification is employed in the neural networks approach for the joint damage assessment of large and complex structures (Koh *et al* 1991).

The noise-injection learning algorithm(Matsuoka 1992) is also used to reduce the noise effects in the modal data. The noise levels included in the training process may be determined by considering the accuracy of each element of the input patterns. In this study, the noise levels for natural frequencies can be taken as smaller than those for the mode shapes.

The effectiveness of the present damage estimation method using neural networks is examined employing the concepts of the mean sizing error, the damage missing error, and the false alarm error (Kim and Stubb, 1996).

4. Numerical example

4. 1 Example Building Structure

A building frame structure shown in Figure 3 is used for the numerical simulation study to examine the

effectiveness of the proposed approach. The beam and column sections are $W24\times55$ and $W14\times145$, the mass density is 7850kg/m^3, and the elastic modulus is $210GPa$. The substructure to be identified consists of six beams and six columns as shown in Figure 3, where the damages are assumed to occur at the ends of the beam members. The intact joint stiffness is assumed to be $3.0\times10^8 N\cdot m/rad$ for all the semi-rigid joints at the ends of the beams. The mode shapes are assumed to be measured only at 15 translational DOF's for the first two mode vectors in the substructure as shown in Figures 4 and 5.

4. 2 Neural Networks Architecture

A four-layer architecture of the NN has been selected from several trials as in Figure 2. The input layer consists of 19 neurons, which include the lower 4 natural frequencies and the 15 translational components of the second mode vectors for the substructure as shown in Figure 5. The first modal data are not used since they are found to have little information on the joint rotational behavior of the substructure. The first hidden and the second hidden layers consist of 15 neurons each. The output layer is composed of 12 joint damage severities. 1500 training patterns have been generated using the Latin hypercube sampling technique based on the assumed probability distributions of the joint damages shown in Figure 6.

4.3 Joint Damage Estimation

The effectiveness of the joint damage assessment using the NN is examined through 500 testing patterns. Several levels of the measurement errors in testing patterns are considered as shown in Table 1. The noise levels included in the training patterns are shown in Table 2. Figure 7 shows that the average value of the mean sizing error over 500 test patterns is about 0.06 for the measurement error level III with moderate noise, when the NN has been trained using the noise injection learning (i.e. NIL-B and NIL-C). It indicates that the neural networks may be reasonably used to assess the damage severities larger than 0.06, but the assessment results for the damage severities smaller than 0.06 may be unreliable. Figure 8 shows that the mean sizing errors for joints 2, 3, 6, 7, 10 and 11 are slightly larger than those for the other joints. It is noteworthy that those are the joints at which four members meet, while only three members meet at the other joints.

The effect of the measurement errors in the testing data set and the effectiveness of the noise injection learning are investigated through the comparisons of the detectability tendencies. The results of the DME and the FAE for various cases are as shown in Figures 9 and 10. It has been observed that the DME reduces very effectively by employing the noise-injection learning for all measurement error cases. For instance, even for the testing data with moderate errors(Case II), the estimated DME's are found to be reasonably small, i.e. $DME \le 0.1$ for the cases where the damage severity is greater than 0.2. This means that 90 percent of the damaged members can be correctly detected. The estimated DME's are almost zero, if the damage severity is greater than 0.3. The results of the FAE also show that the noise-injection learning is very effective to reduce the effects of the measurement noise. In general, the number of the false alarming cases increases, if the testing data contain noise with high level. However, it can be observed that the predicted damaged members whose severities are greater than 0.30 are the truly damaged members in most of the cases, if the noise injection learning with proper levels of noise has been carried out.

5. Experimental Example

5. 1 Experimental Setup

A 2-story frame structure shown in Figure 11 is used in the experimental study. The properties of the beam and column sections are shown in Table 3. The intact joint fixity factors as well as the damaged joint fixity factors are identified using the neural networks approach, because the information of the intact joint stiffness is

inaccessible. The first five natural frequencies and mode shapes are identified at the 8 translational DOF's shown in Figure 11, and the results are used for estimating the unknown fixity factors. Three types of the joint damage are artificially induced; i.e. bolt-missing, L-shape connector-missing, and connector thickness reduction as shown in Figure 12, which represent small, moderate and severe damage cases, respectively.

5. 2 Neural Networks Technique Using Data Perturbation Scheme

A four-layer architecture of the NN has been used, and the input layer consists of 26 neurons, which include the lower 4 natural frequencies, 6 combinations of 4 natural frequencies (e.g. $f_1 f_2, f_1 f_3, \cdots, f_3 f_4$) and 8 translational components of the second and forth mode vectors. The combinations of the natural frequencies are included in the input data to improve the networks performance. The output layer consists of 4 neurons, which represent the joint fixity factors. The first and third mode vectors are not used, since they are not much related to the bending behavior of the beam elements. 1000 training patterns have been numerically generated using the Latin hypercube sampling technique with a uniform probability distribution for the joint damage between 0.0 and 1.0. The noise injection learning's are carried out for three different noise levels: NIL-A, NIL-B, and NIL-C as in Table 2. To improve the estimation for three damage cases shown in Table 4, the data perturbation scheme(Hjelmstad and Shin, 1997) is also incorporated.

5. 3 Joint Damage Estimation

Table 4 shows the estimated joint fixity factors for the intact condition and the estimated joint damage severities for three damage cases. The results are the average values for 100 cases with perturbed modal data for each damage case. The standard deviations are given in the parentheses. In damage case I, one of two connectors is missed at each joint on the first floor. The estimated damage severities for two joints are found to be reasonably consistent in the range of 0.43~0.49, if the noise injection learning has been carried out: i.e. for Cases of NIL-B and NIL-C. However, if the technique has not been used, quite different estimates(0.63 and 0.25) are obtained at two joints with similar damages. It can be also found that the standard deviations of the estimates decrease considerably, if the noise injection learning is carried out. For Damage Case II with a missing connector at Joint 1 and two missing bolts at Joint 4, two damaged joints have been duly detected. The damage severity for the joint with missing bolts is estimated as 0.15, which is less than the value for the joint with a missing connector. For Damage Case III with a reduced connector thickness, the damage severity of the joint has been estimated as approximately 0.9, which means that the joint lost 90% of the initial rotational rigidity. The verification is also performed through the comparisons of the recalculated modal properties using the estimated damage severities with the measured values as in Table 5. It is noteworthy that the modes have been obtained in different order compared with the intact case, particularly for Damage Case I as in Table 5. It is because the damages occur at the joints on the first floor, which have significant affect on the fourth mode. The modal assurance criterion has been employed to rearrange the modes in the input layer of the neural networks to match to those of the intact case. The results show that the recalculated frequencies and mode shapes well agree with the measured values.

6. Conclusions

A method is proposed to estimate the structural joint damages from the modal data using the neural networks technique. The connection stiffness of a beam-to-column joint in a steel frame structure is represented by the stiffness of a zero-length rotational spring at the end of a beam element. The joint damage severity is defined by the reduction ratio of the connection fixity factor. The substructural identification is employed for the local damage assessment in a large and complex structure. Verification of the present method analysis has been carried out through a numerical simulation study on a steel frame with 2-bay and 10-story and also through an

experimental study on a 2-story frame. The results of the joint damage assessment are found to be very reliable even for the cases with severe noise in the input modal data, if the noise injection learning has been carried out with a realistic noise level for each input component: for instance, smaller noise for the natural frequencies and larger noise for the mode shape data. It has been also found that the data perturbation scheme of the modal data can improve the confidence of the estimates for the cases with a small number of the measurement data set.

Acknowledgement

The authors would like to express their sincere appreciation for the financial supports from the Korea Earthquake Engineering Research Center(KEERC) and the Korea Science and Engineering Foundation(KOSEF) to this study.

References

Hjelmstad, Keith D. and Shin, S. (1997), "Damage detection and assessment of structures from static response," *Journal of Engineering Mechanics, ASCE*, **123**(6) 568-576

Matsuoka, K. (1992), "Noise injection into inputs in back-propagation learning", *IEEE Trans. Systems, Man, and Cybernetics*, **22**(3) 436-440

Kim, J.T. and Stubb, N. (1996), "Model Uncertainty Impact and Damage-Detection Accuracy in Plate Girder," *Journal of Structural Engineering, ASCE*, **121**(10) 1409-1417

Koh, C.G., See, L.M., and Balendra, T. (1991), "Estimation of structural parameters in the time domain: a substructural approach," *Earthquake Engineering and Structural Dynamics*, **20**, 787-801

Yun, C.B., Yi, J.H., and Bahng, E.Y.(1998), "Joint Damage Estimation Using Neural Networks," *Proceedings of Fifth Pacific Structural Steel Conference*, 1211-1216

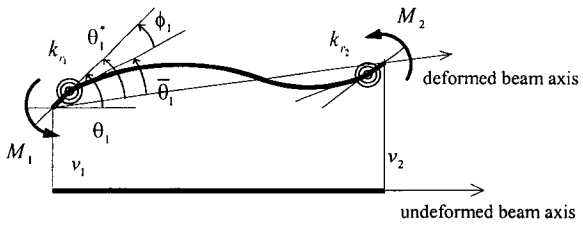

Figure 1. Kinematics of a deformed beam element with semi-rigid connections

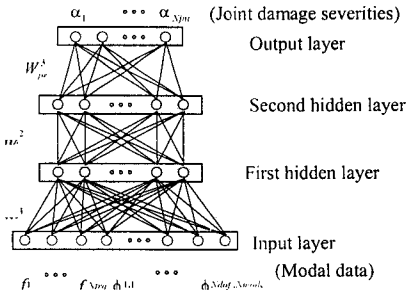

Figure 2. Architecture of back-propagation neural networks

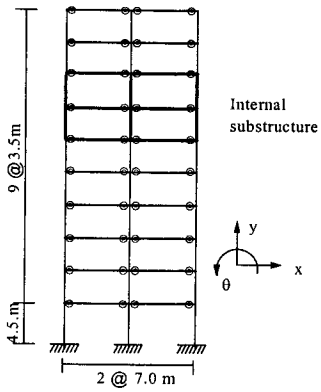

Figure 3. Example structure for analysis

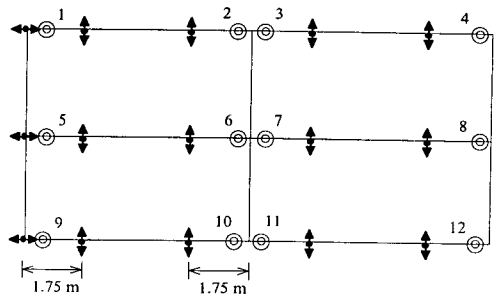

Figure 4. Sensor locations and joint numbers

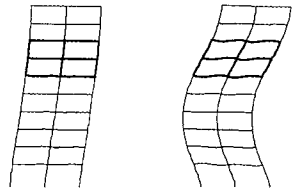

(1.92 Hz)
(a) 1st mode

(5.98 Hz)
(b) 2nd mode

Figure 5. First two mode-shapes

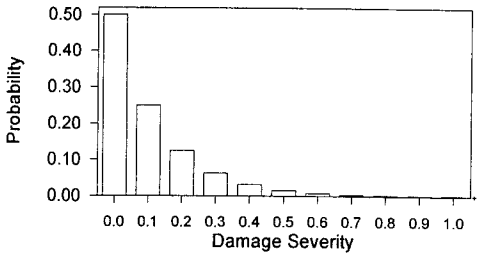

Figure 6. Probability distribution of joint damage

Table 1. Artificial Noises for Simulation of Testing Data (% in RMS level)

Mode No.	I		II		III		IV		V	
	f_i	ϕ_{ii}	f_i	ϕ_{ii}	f_i	ϕ_{ii}	f_i	ϕ_{ii}	f_i	ϕ_{ii}
1	0.0	-	0.2	-	0.3	-	0.5	-	1.0	-
2	0.0	0.0	0.3	5.0	0.5	10.0	1.0	15.0	1.5	20.0
3	0.0	-	0.5	-	1.0	-	1.5	-	2.0	-
4	0.0	-	1.0	-	1.5	-	2.0	-	3.0	-

Table 2. Noise levels for noise-injection learning (% in RMS level)

NIL-A		NIL-B		NIL-C	
f_i	ϕ_{ii}	f_i	ϕ_{ii}	f_i	ϕ_{ii}
0.0	0.0	1.0	10.0	2.0	20.0

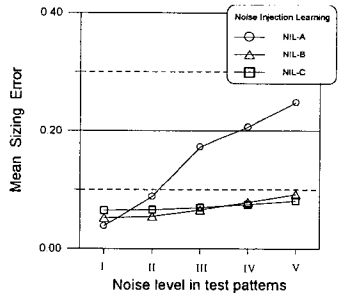

Figure 7. Mean sizing error for different noise levels in test data

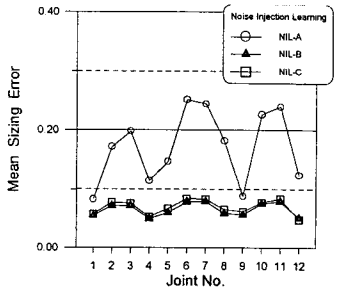

Figure 8. Mean sizing error vs joints (Noise level III in test data)

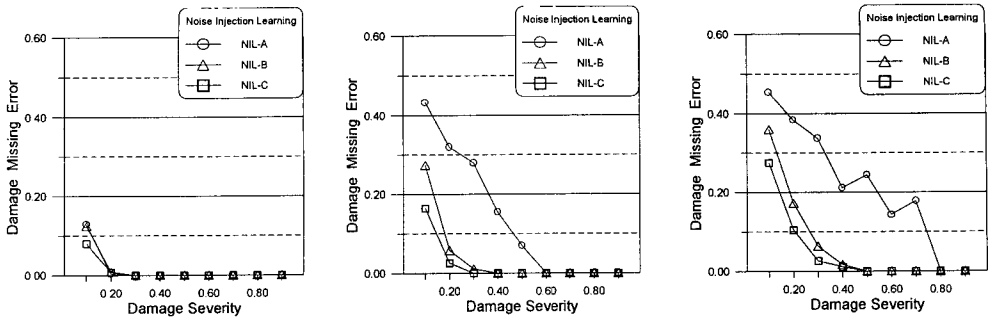

(a) Case I without noise (b) Case III with moderate noise (c) Case V with severe noise

Figure 9. Damage missing error for different noise levels in test data

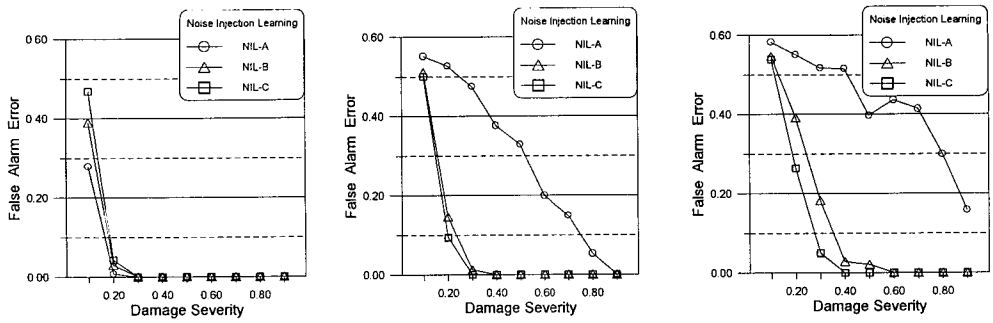

(a) Case I without noise (b) Case III with moderate noise (c) Case V with severe noise

Figure 10. False alarm error for different noise levels in test data

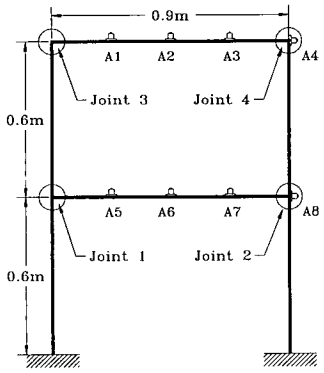

Figure 11. Test structure

Table 3. Structural properties of test structure

Cases	A (m^2)	I (m^4)	E (Pa)	ρ (kg/m^3)
Beam	$8.69x10^{-4}$	$5.48x10^{-9}$	$2.10x10^{11}$	7850
Column	$4.30x10^{-4}$	$6.62x10^{-10}$		

Note : Mass of each accelerometer is 76.85g.

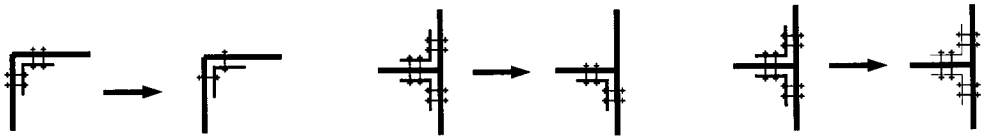

(a) Bolt missing (b) Connector missing (c) Connector thickness reduction

Figure 12. Artificially induced joint damages

Table 4. Estimated joint damage severities

Cases \ Joint No.			1	2	3	4
Intact	$\gamma_{0,i}$		1.00	0.94	0.70	0.63
	$\alpha_{0,i}$		0.00	0.00	0.00	0.00
I	Damage Type		Conn missing	Conn missing	-	-
	α_i	NIL-A	0.63(0.32)	0.25(0.32)	0.00(0.05)	0.00(0.20)
		NIL-B	0.43(0.03)	0.49(0.04)	0.00(0.02)	0.00(0.02)
		NIL-C	0.48(0.06)	0.45(0.04)	0.00(0.01)	0.00(0.01)
II	Damage Type		Conn missing	-	-	Bolt missing
	α_i	NIL-A	0.33(0.22)	0.08(0.02)	0.14(0.18)	0.21(0.33)
		NIL-B	0.39(0.07)	0.05(0.05)	0.00(0.03)	0.16(0.03)
		NIL-C	0.34(0.06)	0.06(0.04)	0.00(0.02)	0.15(0.01)
III	Damage Type		-	-	Conn thick reduc	-
	α_i	NIL-A	0.05(0.11)	0.05(0.17)	0.98(0.24)	0.19(0.32)
		NIL-B	0.07(0.05)	0.09(0.04)	0.88(0.09)	0.05(0.06)
		NIL-C	0.06(0.03)	0.06(0.03)	0.86(0.09)	0.06(0.04)

Note: Values in the parentheses are the standard deviations of the estimated damage severities.

Table 5. Comparisons of measured and recalculated natural frequencies

Cases \ Mode No.		1			2			3			4		
		f_{mea} (Hz)	f_{recal} (Hz)	Error (%)	f_{mea} (Hz)	f_{recal} (Hz)	Error (%)	f_{mea} (Hz)	f_{recal} (Hz)	Error (%)	f_{mea} (Hz)	f_{recal} (Hz)	Error (%)
Intact		4.59	4.58	0.04	18.96	18.73	1.21	22.26	21.57	3.09	25.83	25.22	2.74
I	NIL-A	4.22	4.25	0.71	18.83	18.91	0.42	22.27	21.37	4.04	17.32	17.59	1.55
	NIL-B		4.17	1.18		18.52	1.64		21.41	3.86		16.88	2.54
	NIL-C		4.26	0.95		18.52	1.64		21.32	4.26		17.21	0.63
II	NIL-A	4.34	4.34	0.00	18.81	17.11	9.04	22.30	21.61	3.09	20.83	21.04	1.01
	NIL-B		4.28	1.38		18.24	3.03		21.77	2.37		20.41	2.01
	NIL-C		4.41	1.61		18.29	2.76		21.26	4.66		21.52	3.31
III	NIL-A	4.24	4.17	1.65	14.71	14.50	1.43	21.85	20.87	4.48	24.31	24.17	0.57
	NIL-B		4.26	0.47		15.25	3.67		21.43	1.92		23.50	3.30
	NIL-C		4.28	0.94		15.36	4.41		21.51	1.55		23.92	1.60

Note 1. NIL-A, NIL-B, and NIL-C denote the cases of noise injection learning described in Table 2.

2. f_{mea} and f_{recal} are the measured and recalculated natural frequencies.

3. Error = $| f_{mea} - f_{recal} | / f_{mea} \times 100$